

# Cellular glutathione peroxidase deficiency and endothelial dysfunction

MARC A. FORGIONE,<sup>1,2\*</sup> NORBERT WEISS,<sup>2\*</sup> STANLEY HEYDRICK,<sup>2</sup> ANDRÉ CAP,<sup>2</sup>  
ELIZABETH S. KLINGS,<sup>1,3</sup> CHARLENE BIERL,<sup>2</sup> ROBERT T. EBERHARDT,<sup>1,2</sup>  
HARRISON W. FARBER,<sup>1,3</sup> AND JOSEPH LOSCALZO<sup>1,2</sup>

<sup>1</sup>Evans Department of Medicine, <sup>2</sup>Whitaker Cardiovascular Institute, Department of Pharmacology, and <sup>3</sup>Pulmonary Center, Boston University School of Medicine, Boston, Massachusetts 02118

Received 10 July 2001; accepted in final form 19 November 2001

**Forgione, Marc A., Norbert Weiss, Stanley Heydrick, André Cap, Elizabeth S. Klings, Charlene Bierl, Robert T. Eberhardt, Harrison W. Farber, and Joseph Loscalzo.** Cellular glutathione peroxidase deficiency and endothelial dysfunction. *Am J Physiol Heart Circ Physiol* 282: H1255–H1261, 2002. First published December 6, 2001; 10.1152/ajpheart.00598.2001.—Cellular glutathione peroxidase (GPx-1) is the most abundant intracellular isoform of the GPx antioxidant enzyme family. In this study, we hypothesized that GPx-1 deficiency directly induces an increase in vascular oxidant stress, with resulting endothelial dysfunction. We studied vascular function in a murine model of homozygous deficiency of GPx-1 (GPx-1<sup>-/-</sup>). Mesenteric arterioles of GPx-1<sup>-/-</sup> mice demonstrated paradoxical vasoconstriction to  $\beta$ -methacholine and bradykinin, whereas wild-type (WT) mice showed dose-dependent vasodilation in response to both agonists. One week of treatment of GPx-1<sup>-/-</sup> mice with L-2-oxothiazolidine-4-carboxylic acid (OTC), which increases intracellular thiol pools, resulted in restoration of normal vascular reactivity in the mesenteric bed of GPx-1<sup>-/-</sup> mice. We observed an increase of the isoprostane iPF<sub>2 $\alpha$</sub> -III, a marker of oxidant stress, in the plasma and aortas of GPx-1<sup>-/-</sup> mice compared with WT mice, which returned toward normal after OTC treatment. Aortic sections from GPx-1<sup>-/-</sup> mice showed increased binding of an anti-3-nitrotyrosine antibody in the absence of frank vascular lesions. These findings demonstrate that homozygous deficiency of GPx-1 leads to impaired endothelium-dependent vasodilator function presumably due to a decrease in bioavailable nitric oxide and to increased vascular oxidant stress. These vascular abnormalities can be attenuated by increasing bioavailable intracellular thiol pools.

nitric oxide; peroxynitrite; oxidant stress

NITRIC OXIDE (NO) synthesized by the endothelium contributes to vascular tone (23), preserves endothelial integrity (13), inhibits smooth muscle cell migration and proliferation (16), and acts as an antioxidant (30). An increase in reactive oxygen species (ROS), leading to increased oxidant stress in the vasculature, promotes endothelial dysfunction (28) associated with NO insufficiency (15).

The enzyme glutathione peroxidase (GPx) is a selenocysteine-containing protein that serves an important role in the cellular defense against oxidant stress (24) by utilizing reduced glutathione (GSH) to reduce hydrogen peroxide (H<sub>2</sub>O<sub>2</sub>) and lipid peroxides to their corresponding alcohols (37). GPx exists in several isoforms, and the most abundant intracellular isoform is cellular GPx, or GPx-1. We (7, 36, 39) have previously shown that elevated homocysteine concentrations suppress GPx-1 expression in endothelial cells in vitro and in mildly hyperhomocysteinemic mice in vivo and suggested that this effect may account, in part, for the vascular oxidant stress of hyperhomocysteinemic states. Hydrogen peroxide forms the toxic oxygen species hydroxyl radical ( $\cdot$ OH), which is highly reactive and causes lipid peroxidation, and hydroxide anion (OH<sup>-</sup>), which promotes alkaline tissue damage, a process that is offset in part by catalase and GPx-1-dependent reduction to H<sub>2</sub>O. Elevated levels of lipid peroxides are accompanied by an increase in peroxyl radicals, which can inactivate NO through the formation of lipid peroxynitrites (19, 30), although the precise molecular mechanism(s) by which these peroxyl radicals form remains speculative (19). Thus a deficiency of GPx-1 would theoretically lead to an increase in ROS and a decrease in bioavailable NO.

Because GSH represents one of the most important intracellular antioxidants, primarily as a cosubstrate for GPx-1, we hypothesized that this antioxidant system plays a central role in protecting the vasculature in states of increased oxidant stress. To test the hypothesis, we studied the role of this system in modulating endothelial function by using a murine model of targeted gene disruption of the GPx-1 gene.

## MATERIALS AND METHODS

**Reagents and animals.** All chemicals were obtained from Sigma (St. Louis, MO) unless otherwise stated. Mice homozygous for disruption of the GPx-1 gene (GPx-1<sup>-/-</sup> mice) were kindly provided by Dr. Y. Ho (Wayne State University; Detroit, MI) and subsequently bred at our institution. GPx-1

\*M. A. Forgione and N. Weiss contributed equally to this work.

Address for reprint requests and other correspondence: J. Loscalzo, Boston Univ. School of Medicine, 715 Albany St., W507, Boston, MA 02118 (E-mail: jloscalz@bu.edu).

The costs of publication of this article were defrayed in part by the payment of page charges. The article must therefore be hereby marked "advertisement" in accordance with 18 U.S.C. Section 1734 solely to indicate this fact.

was inactivated by insertion of a neomycin resistance gene (NEO) cassette into an *EcoRI* site located in exon 2 of the GPx-1 gene, which was then inserted into mouse embryonic stem cells as previously described (11).

Homozygous GPx-1-deficient mice and wild-type (WT; +/+) control mice were used at 16–20 wk of age for the experiments assessing vascular function and at 16 to 20 and 40 wk to evaluate markers of oxidant stress. The animals were fed standard chow and handled according to National Institutes of Health guidelines.

L-2-Oxothiazolidine carboxylic acid (OTC) was administered to the animals in water bottles at a concentration of  $2 \mu\text{mol} \cdot \text{g}^{-1} \cdot \text{day}^{-1}$ , a dose known to affect hepatic GSH levels. Actual ingestion was determined by weighing the drinking bottles daily.

All mice were killed during full anesthesia with pentobarbital by exsanguination during the collection of blood and tissue. All procedures were approved by the Institutional Animal Care and Use Committee at Boston University Medical Center.

**Genotype determination.** DNA was obtained by extraction from mouse tail snips. DNA ( $1 \mu\text{l}$ ) was amplified in a 50- $\mu\text{l}$  PCR reaction containing 10 mM Tris·HCl (pH 8.3), 50 mM KCl, 1.5 mM MgCl<sub>2</sub>, 0.001% gelatin, 0.1 mM dNTP, and 0.18  $\mu\text{M}$  each primer. To identify the WT GPx-1 gene, we utilized the forward primer FinN (5'-GTTTCCCGTGCAATCAGTTCG-3') and the reverse primer R<sub>3</sub>N (5'-TCGGACGTACCCTTGAGGGAAT-3') to detect the presence of a 293-bp fragment. To identify GPx-1<sup>-/-</sup> mice, we used FinN and RpgkN (5'-CATTTGTCACGTCCTGCAC-3') as the reverse primer to amplify a 509-bp fragment in the NEO insert. Reaction products were analyzed by electrophoresis on a 1% agarose gel. GPx-1<sup>-/-</sup> mice were identified by an exclusive 509-bp product, and WT mice were identified by an exclusive 293-bp product.

**Hepatic GPx-1 activity.** Liver samples were snap-frozen in liquid nitrogen and stored at  $-80^{\circ}\text{C}$ . Tissue (0.5 g) was homogenized in an ice-cold buffer containing 50 mM Tris (pH 7.5), 5 mM EDTA (pH 8), and 1 mM dithiothreitol (DTT). The homogenate was centrifuged at 10,000  $g$  for 20 min at  $4^{\circ}\text{C}$ . GPx activity was then determined from the supernatant by coupling the reduction of peroxides and the oxidation of glutathione with the reduction of oxidized glutathione by glutathione reductase using NADPH as a cofactor (9). The reaction was carried out in a buffer containing 50 mM Tris·HCl, 5 mM EDTA, 1 mM glutathione, 0.4 U/ml glutathione reductase, and 0.2 mM NADPH (pH 7.6) and initiated by the addition of tert-butyl-hydroperoxide (0.22 mM final concentration). GPx activity was monitored by a decrease in light absorbance with oxidation of NADPH at 340 nm. Enzyme activity was calculated using a molar extinction coefficient for NADPH of  $6,220 \text{ M}^{-1} \cdot \text{cm}^{-1}$  and normalized to protein concentration.

**Mesenteric microcirculation studies.** Vascular reactivity in the mesenteric circulation in response to the endothelium-dependent agonists  $\beta$ -methacholine (BMC) and bradykinin (BK) and the endothelium-independent vasodilator sodium nitroprusside (SNP) was assessed in vivo using videomicroscopy as previously described (7, 35).

**cGMP levels.** cGMP content was measured in isolated thoracic aortas as previously described (2) with slight modifications. In anesthetized mice, the aortas were gently and antegradely perfused with normal saline via puncture of the left ventricle, the thoracic aortas were then excised, and loose connective tissue of the adventitia was removed. The tissue was weighed, placed in Dulbecco's PBS containing Ca<sup>2+</sup> and Mg<sup>2+</sup> (GIBCO-BRL Life Technologies, distributed by Invitro-

gen; Carlsbad, CA), and then supplemented with 0.068 mM EDTA, 0.14 mM ascorbate, and 11.1 mM glucose. The vessels were preincubated at  $37^{\circ}\text{C}$ , aerated with 95% O<sub>2</sub>-5% CO<sub>2</sub> for 15 min, stimulated with BK ( $10^{-5}$  M) for 1 min, snap-frozen in liquid nitrogen, and then stored at  $-80^{\circ}\text{C}$  until analysis. The tissue was homogenized in ice-cold 50 mM phosphate buffer containing 7.5% (vol/vol) trichloroacetic acid and centrifuged at 2,000  $g$  for 10 min at  $4^{\circ}\text{C}$ . Trichloroacetic acid was removed from the supernatant by extraction with water-saturated diethyl ether. cGMP content in the supernatant was then measured using a commercially available immunoassay (Cayman Chemical; Ann Arbor, MI) according to the manufacturer's instructions.

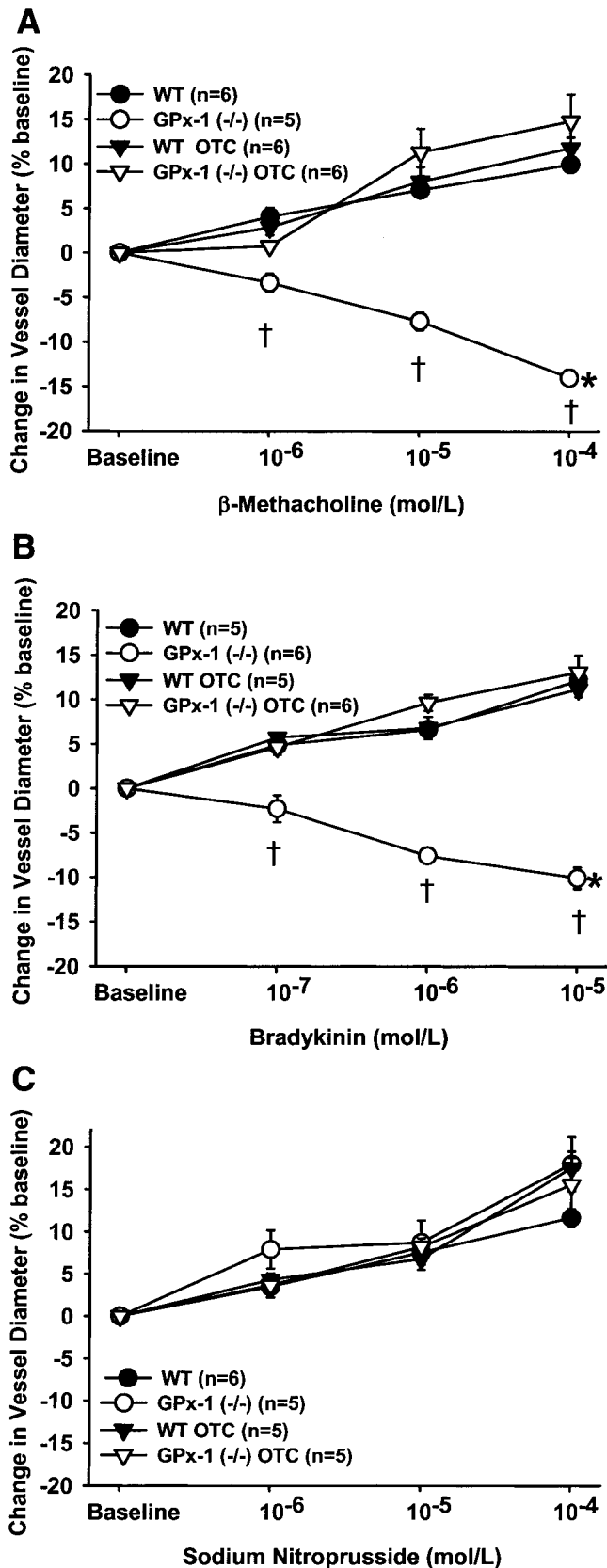
**Aortic endothelial NO synthase expression.** Expression of endothelial NO synthase (eNOS) in aortic tissue was assessed by immunoblot analysis. Thoracic aortas were homogenized in 50 mM Tris·HCl buffer (pH 7.5) in the presence of EDTA (2 mM) and protease inhibitors (1  $\mu\text{g}/\text{ml}$  aprotinin, 10  $\mu\text{g}/\text{ml}$  pepstatin, 10  $\mu\text{g}/\text{ml}$  leupeptin, 1 mM benzamide, and 1 mM phenylmethylsulfonyl fluoride) and adjusted to equal protein concentrations in the same buffer. Samples were reduced and denatured by adding DTT (0.05 M final concentration) and lithium dodecyl sulfate sample buffer (Invitrogen) and by boiling for 5 min. Samples of 10  $\mu\text{g}$  protein each were electrophoresed through Bis-Tris·HCl-buffered (pH 6.4) 12% polyacrylamide gels (NuPAGE, Invitrogen) and blotted on nitrocellulose filters. Blots were blocked in 5% skimmed milk in PBS-Tween (PBS-T;  $1 \times$  PBS + 0.05% Tween) for at least 15 min, followed by an overnight incubation with a monoclonal antibody to eNOS (1:1,000, Signal Transduction Laboratories; Lexington, KY). Blots were washed three times for at least 15 min each in PBS-T and then incubated with a peroxidase-conjugated second antibody for 1 h (1:2,500, Signal Transduction Laboratories). Immunoblots were developed using the enhanced chemiluminescence detection system (Amersham Pharmacia Biotech; Piscataway, NJ). Equal loading of protein was confirmed by staining parallel gels with Coomassie brilliant blue or the filters with Ponceau S.

**Plasma and tissue isoprostane determination.** Mice were killed and plasma was obtained by centrifugation of blood collected in tubes containing a final concentration of 0.1 M EDTA, snap-frozen in liquid nitrogen, and stored at  $-80^{\circ}\text{C}$ . Tissue samples were weighed as described previously (7), snap-frozen in liquid nitrogen, and stored at  $-80^{\circ}\text{C}$ .

The isoprostane iPF<sub>2 $\alpha$</sub> -III was purified from plasma samples. Plasma was diluted 1:15 in ultrapure water, and samples were applied to a reverse-phase C-18 column (Alltech; Deerfield, IL) at pH 3 and eluted with 1:1 (vol/vol) ethyl acetate-heptane. The eluant was then further purified on a Silica column (Alltech) and eluted with 1:1 (vol/vol) ethyl acetate-methanol. iPF<sub>2 $\alpha$</sub> -III was measured from the eluant using a commercially available immunoassay (Cayman Chemical).

Tissue samples were minced, and iPF<sub>2 $\alpha$</sub> -III was extracted overnight using 2:1 (vol/vol) chloroform-methanol with 0.0005% butylated hydroxytoluene. Samples were filtered through glass wool, and the organic phase was evaporated at  $40^{\circ}\text{C}$  under nitrogen. The dried sample was resuspended in methanol, saponified using 15% KOH, and then incubated for 60 min at  $40^{\circ}\text{C}$ . The sample was then adjusted to pH 2 and applied to the C-18 column as above. iPF<sub>2 $\alpha$</sub> -III was assayed from the eluant of the C-18 column as described above.

**Tissue phospholipid hydroperoxide content.** Measurement of phospholipid hydroperoxide levels in hepatic tissue was performed by HPLC using a LC-Si column as previously described (32).



**Histological assessment.** Tissue, including the heart, aorta, and mesentery, was excised from GPx-1<sup>-/-</sup> and WT mice. The tissues were fixed in 4% formalin, embedded in paraffin, and stained with hematoxylin and eosin as well as Masson trichrome.

**Immunohistochemistry for 3-nitrotyrosine.** The production of reactive nitrogen species was assessed in aortic tissue by the presence of the stable endproduct of their interaction with cellular tyrosine residues, 3-nitrotyrosine, as previously described (7, 10).

**Data analysis.** Continuous data are expressed as means  $\pm$  SE. The Kruskal-Wallis test was used for multigroup comparisons of continuous variables, followed by Mann-Whitney *U*-tests to compare differences between two groups. Differences in the dose response to agonists between groups were tested using two-way repeated-measures ANOVA with post hoc analysis performed using Scheffé's *F*-test and Bonferroni-Dunn methods. Statistical significance was defined as a *P* value  $< 0.05$ .

## RESULTS

**Hepatic GPx-1 activity.** Hepatic cellular GPx activity was undetectable in GPx-1<sup>-/-</sup> mice compared with WT mice ( $-1.5 \pm 0.9$  vs.  $579.4 \pm 6.1$  mU/mg protein, *P*  $< 0.0001$ ).

**Mesenteric vascular reactivity.** Superfusion with BMC and BK produced dose-dependent vasodilation of mesenteric arterioles in WT mice, with a maximal vascular response (MVR) of  $10.0 \pm 0.7\%$  (BMC) and  $12.2 \pm 1.3\%$  (BK), respectively, at concentrations of  $10^{-4}$  M and  $10^{-5}$  M, respectively. However, superfusion of mesentery from GPx-1<sup>-/-</sup> mice with either endothelium-dependent agonist resulted in paradoxical arteriolar vasoconstriction, with a MVR of  $-14.0 \pm 0.7\%$  (BMC) and  $-10.1 \pm 1.2\%$  (BK), respectively (Fig. 1, A and B), that was statistically different from the response of WT mice (*P*  $< 0.0001$ ). Superfusion of the mesentery with SNP resulted in dose-dependent arteriolar vasodilation that was similar in the two groups of animals (Fig. 1C). These results indicate that GPx-1<sup>-/-</sup> mice have impaired endothelium-dependent vasodilation and intact endothelium-independent vasodilation in mesenteric arterioles, suggesting a depletion of bioavailable NO.

**Aortic cGMP levels and eNOS expression.** Aortic tissue from GPx-1<sup>-/-</sup> mice tended to accumulate less cGMP upon stimulation with bradykinin for 1 min compared with aortic tissue from WT mice ( $0.38 \pm 0.07$  vs.  $0.80 \pm 0.12$  pmol/ml tissue, *P*  $< 0.02$ ; Fig. 2). This effect was independent of aortic eNOS expression because immunoblot analysis of eNOS protein did not show any appreciable difference between GPx-1<sup>-/-</sup> and WT mice (data not shown).

**Isoprostanes/hepatic phospholipid hydroperoxides.** iPF<sub>2 $\alpha$</sub> -III levels were elevated in the plasma and aortas of 16- to 20-wk-old GPx-1<sup>-/-</sup> mice compared with WT

Fig. 1. Mesenteric microvascular response to superfusion of  $\beta$ -methacholine (A), bradykinin (B), and sodium nitroprusside (C) in wild-type (WT) mice, WT mice treated with L-2-oxothiazolidine carboxylic acid (OCT), glutathione peroxidase-deficient (GPx-1<sup>-/-</sup>) mice, and GPx-1<sup>-/-</sup> mice treated with OCT. \**P*  $< 0.0001$  compared with WT mice for the entire dose response; †*P*  $< 0.01$  compared with WT mice at each specific concentration of agonist.

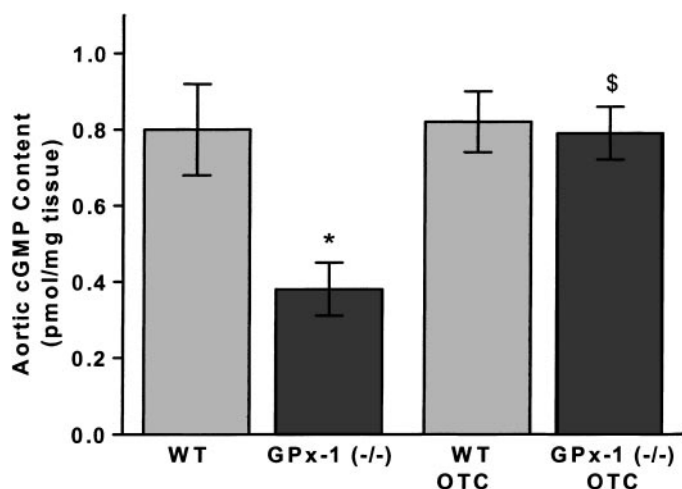


Fig. 2. Aortic cGMP accumulation stimulated with bradykinin for 1 min in WT mice ( $n = 8$ ), GPx-1<sup>-/-</sup> mice ( $n = 8$ ), WT treated with OTC ( $n = 8$ ), and GPx-1<sup>-/-</sup> mice treated with OTC ( $n = 8$ ). \* $P < 0.02$  compared with WT mice; \$ $P < 0.02$  compared with GPx-1<sup>-/-</sup>.

mice [plasma:  $168.4 \pm 25.4$  vs.  $84.6 \pm 7.6$  pg/ml,  $n = 6$  mice/group,  $P < 0.005$  (Fig. 3A); and aortas:  $13.3 \pm 2.8$  vs.  $8.4 \pm 1.1$  pg/mg tissue,  $n = 6$  mice/group,  $P < 0.01$  (Fig. 3B)]. By 40 wk of age, plasma iPF<sub>2 $\alpha$</sub> -III increased further to  $214.0 \pm 18.0$  pg/ml in GPx-1<sup>-/-</sup> and  $100.5 \pm 5.4$  pg/ml in WT mice ( $n = 6$  mice/group,  $P < 0.001$ ). Aortic iPF<sub>2 $\alpha$</sub> -III levels did not increase further ( $14.9 \pm 1.8$  vs.  $8.2 \pm 0.5$  pg/mg tissue, respectively, for GPx-1<sup>-/-</sup> and WT mice,  $n = 6$  mice/group,  $P < 0.01$ ). Cardiac iPF<sub>2 $\alpha$</sub> -III also increased in GPx-1<sup>-/-</sup> mice compared with WT mice ( $17.2 \pm 0.4$  vs.  $5.6 \pm 1.1$  pg/mg tissue,  $n = 6$  mice/group,  $P < 0.001$ ), as did hepatic iPF<sub>2 $\alpha$</sub> -III levels ( $1.8 \pm 0.2$  pg/mg tissue for GPx-1<sup>-/-</sup> mice vs.  $0.6 \pm 0.2$  pg/mg tissue for WT mice,  $n = 6$  mice/group,  $P < 0.01$ ). Hepatic phospholipid hydroperoxides were also elevated in GPx-1<sup>-/-</sup> mice compared with WT mice almost twofold ( $199 \pm 31\%$  vs.  $100 \pm 9\%$ ,  $n = 6$  mice/group,  $P < 0.05$ ).

**Effect of OTC treatment.** Treatment of mice with OTC resulted in an increase in hepatic GPx-1 activity in WT mice ( $679.4 \pm 17.6$  vs.  $579.4 \pm 6.1$  mU/mg protein for untreated,  $P < 0.01$ ) but did not affect enzyme activity in GPx-1<sup>-/-</sup> mice ( $1.7 \pm 2.5$  vs.  $-1.5 \pm 0.9$  mU/mg protein for untreated).

OTC treatment of GPx-1<sup>-/-</sup> mice restored normal dose-dependent arteriolar vasodilation to BMC (MVR =  $14.8 \pm 3.0\%$ ) and BK (MVR =  $13.1 \pm 1.9\%$ ), which was similar to the response observed in WT mice treated with OTC (MVR =  $11.8 \pm 9\%$  for BMC and  $11.2 \pm 0.9\%$  for BK; Fig. 1, A and B). There was no significant difference in the vascular reactivity with superfusion of SNP in either group of mice (Fig. 1C).

GPx-1<sup>-/-</sup> mice tended to accumulate less cGMP in aortic tissue compared with WT mice. cGMP levels in aortic tissue from OTC-treated GPx-1<sup>-/-</sup> mice ( $0.082 \pm 0.08$  pmol/mg tissue), however, were not different from the levels in WT mice and in OTC-treated WT mice ( $0.79 \pm 0.07$  pmol/mg tissue; Fig. 2). OTC treatment did not affect aortic eNOS expression, which was sim-

ilar in WT and GPx-1<sup>-/-</sup> mice without and with OTC treatment (data not shown).

OTC treatment also resulted in a significant reduction of plasma iPF<sub>2 $\alpha$</sub> -III ( $96.7 \pm 16.0$  pg/ml,  $P < 0.05$  compared with untreated GPx-1<sup>-/-</sup> mice; Fig. 3A) and a trend to reduction in aortic iPF<sub>2 $\alpha$</sub> -III ( $8.7 \pm 3.4$  pg/mg tissue for OTC-treated GPx-1<sup>-/-</sup> mice vs.  $13.3 \pm 2.8$  pg/mg tissue for untreated GPx-1<sup>-/-</sup> mice,  $P = 0.074$ ; Fig. 3B).

**Histological assessment and 3-nitrotyrosine staining.** There were no appreciable differences in aortic morphology by hematoxylin and eosin or Masson trichrome staining in the GPx-1<sup>-/-</sup> mice compared with WT mice. However, immunostaining of aortic tissue with an 3-nitrotyrosine antibody showed greater staining for 3-nitrotyrosine in GPx-1<sup>-/-</sup> mice compared with WT mice (Fig. 4). This increase in staining was primarily on the endothelial surface and adventitia, supporting increased reactive nitrogen species formation at these sites.

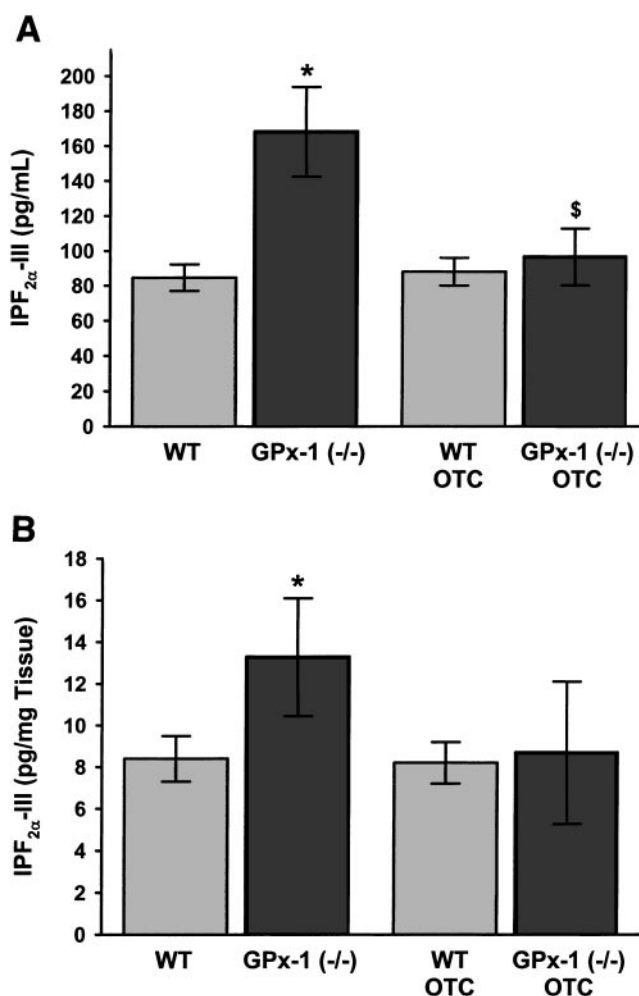


Fig. 3. iPF<sub>2 $\alpha$</sub> -III levels in plasma (A) and aortas (B) from WT mice, GPx-1<sup>-/-</sup> mice, WT mice treated with OTC, and GPx-1<sup>-/-</sup> mice treated with OTC;  $n = 6$  mice/group. \* $P < 0.005$  compared with WT mice; § $P < 0.05$  compared with GPx-1<sup>-/-</sup> mice.

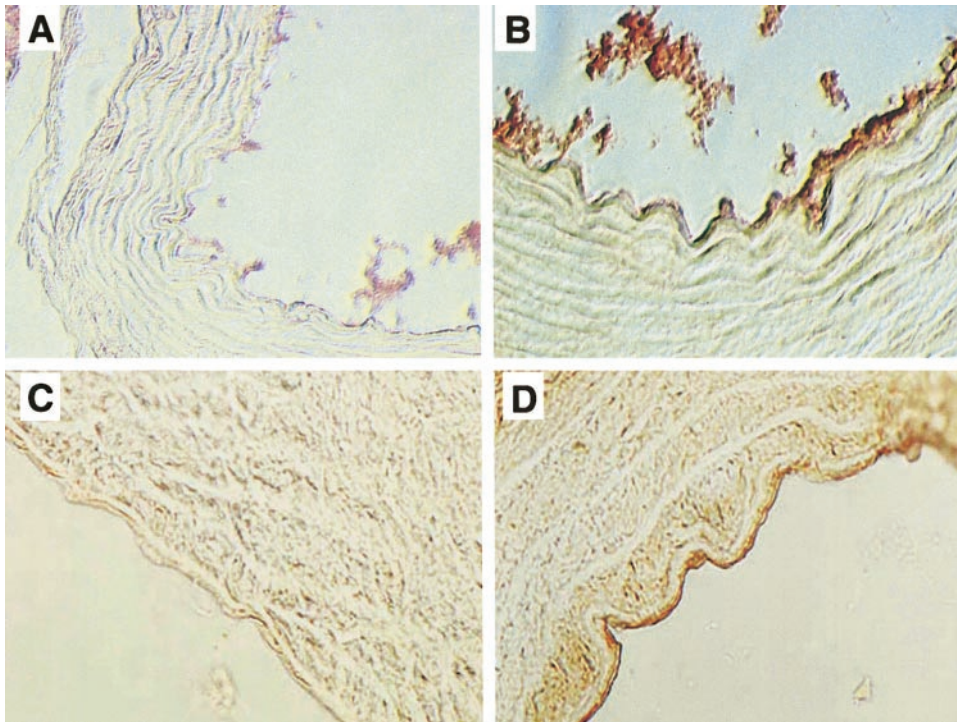


Fig. 4. Cross sections of the aortic arch stained for 3-nitrotyrosine in animals at 10 wk of age. *A*: WT with primary antibody; *B*: WT preincubated with peroxynitrite (positive control); *C*: GPx-1<sup>-/-</sup> without primary antibody (negative control); *D*: GPx-1<sup>-/-</sup> with primary antibody.

## DISCUSSION

We found that homozygous deficiency of the GPx-1 gene produces vascular dysfunction as well as oxidative and nitrosative stress. The vascular dysfunction we observed was detected in response to mesenteric superfusion with BMC and BK, not SNP, indicating that the aberrant microvascular function is endothelium dependent. The trend to lower cGMP accumulation in aortic tissue from GPx-1<sup>-/-</sup> mice after stimulation with BK indicates a decrease in bioavailable endothelium-derived NO, which is not caused by decreased expression of eNOS protein, as indicated by immunoblot analysis.

NO plays a critical role in the endothelial response to muscarinic agonists (20). In normal arteries, muscarinic agonists stimulate NO release, which attenuates the muscarinic agonist-induced vasoconstrictor effect and causes vascular relaxation. However, with a depletion of bioavailable NO in the presence of increased oxidant stress, vasoconstriction occurs because there is unopposed muscarinic stimulation of vascular smooth muscle cells. Abnormal endothelial responses to muscarinic agonists have been shown to be a marker for the development of atherothrombosis (18) as well as a risk factor for a worse prognosis in the presence of atherosclerotic vascular disease (18, 31, 34). Because endothelial response to a direct vasodilator, SNP, was similar between both groups, we can infer that the effect of endothelial dysfunction from homozygous GPx-1 deficiency is not a consequence of impaired vascular smooth muscular function. Therefore, a depletion of bioavailable NO likely plays a role in the endothelial dysfunction that occurs in GPx-1 deficiency. Importantly, this dysfunction occurs in the absence of frank

structural vascular lesions, suggesting that the endothelial dysfunction may precede the development of vascular lesions.

Because GPx-1 plays a central role in defending the cell from ROS, its deficiency should lead to increased oxidant stress in the cell. GPx-1 has a much higher Michaelis-Menten constant for H<sub>2</sub>O<sub>2</sub> than catalase (12), the other important cellular enzyme involved in the detoxification of H<sub>2</sub>O<sub>2</sub>. In endothelial cells, 70% of H<sub>2</sub>O<sub>2</sub> generated by activated polymorphonuclear leukocytes is detoxified by GPx-1 (6); importantly, there is no change in catalase activity in GPx-1<sup>-/-</sup> mice (11). Chemical inhibition of GPx-1 activity in macrophages results in increased cellular peroxide formation and increased superoxide (O<sub>2</sub><sup>-•</sup>) production (27). GPx-1<sup>-/-</sup> mice have decreased survival compared with WT mice after a lethal injection of the xenobiotic paraquat (3), which induces formation of O<sub>2</sub><sup>-•</sup> and H<sub>2</sub>O<sub>2</sub>, indicating an impaired ability to detoxify ROS.

Increased ROS in the presence of GPx-1 deficiency induces lipid peroxidation, which we evaluated by measuring the isoprostane iPF<sub>2α</sub>-III and hepatic phospholipid hydroperoxides. Isoprostanes are formed largely (but not exclusively) from the non-cyclooxygenase (COX)-dependent peroxidation of arachidonic acid (14, 22) and serve as an index of oxidant stress. The isoprostane iPF<sub>2α</sub>-III has been shown to be elevated in several conditions associated with endothelial dysfunction, such as diabetes mellitus (5) and hypercholesterolemia (4, 26). Isoprostanes may contribute to vascular pathology by serving as mitogens (14) and vasoconstrictors (22). There is some capacity for iPF<sub>2α</sub>-III to form in a COX-dependent fashion; however, urinary iPF<sub>2α</sub>-III excretion in diabetics (5) was unaffected by

the administration of a reversible or an irreversible COX inhibitor, whereas urinary 11-dehydro-thromboxane B<sub>2</sub> (a thromboxane metabolite that depends on COX for its formation) excretion was decreased. Riley and colleagues (25) have demonstrated similar results using an irreversible COX inhibitor in cigarette smokers (25), as has McAdam and co-workers (17) in normal volunteers given endotoxin. Thus the enzymatic formation of isoprostanes may be of little relevance in vivo. GPx-1<sup>-/-</sup> mice had significantly increased levels of iPF<sub>2α</sub>-III compared with WT mice in aortic tissue and plasma. GPx-1<sup>-/-</sup> mice also had increased phospholipid hydroperoxide levels in the liver compared with WT mice, consistent with a previous report (8) of GPx-1 deficiency that was generated in a different fashion than this model. These two indexes of lipid peroxidation reflect the increased oxidant stress occurring throughout the lifetime of these animals and may contribute to the aforementioned endothelial dysfunction.

Peroxynitrite (ONOO<sup>-</sup>) and peroxynitrous acid are potent oxidants and reactive nitrogen species that are formed from the reaction of NO with O<sub>2</sub><sup>•-</sup>. Peroxynitrite has a short half-life (29), which makes its detection difficult in biological systems, and reacts with cellular tyrosine residue to form the stable 3-nitrotyrosine derivative. We detected increased immunostaining for 3-nitrotyrosine in aortic tissue of GPx-1<sup>-/-</sup> mice compared with WT mice. GSH has been shown in vitro to be dependent on GPx to defend against peroxynitrite toxicity (peroxynitrite reductase activity) (33); our observations suggest the same in vivo, because these immunostaining experiments show that there is increased nitrosative stress in GPx-1<sup>-/-</sup> mice.

The administration of OTC increases hepatic GSH (41), cysteine, and glutathione levels in vascular tissue, plasma (1), and lymphocytes (21) as well as total blood cysteine concentration (38). OTC is transported into cells and converted to cysteine by the enzyme 5-oxo-prolinase (40); thus OTC represents an effective way to increase intracellular thiol pools.

OTC treatment reversed the vasoconstrictor response to superfusion with BMC and BK observed in the mesenteric bed of GPx-1<sup>-/-</sup> mice and the decrease in aortic cGMP accumulation after stimulation with BK, indicating an increase in bioavailable NO. Vita and colleagues (38) have reported an improvement in NO-dependent brachial artery responses to shear stress as measured by ultrasound after OTC treatment in patients with coronary artery disease. OTC treatment also decreased plasma iPF<sub>2α</sub>-III and demonstrated a trend toward a decrease of aortic iPF<sub>2α</sub>-III in GPx-1<sup>-/-</sup> mice. Preliminary data show that OTC treatment significantly increased total low-molecular-weight thiols in cardiac tissue extracts by 36% from GPx-1<sup>-/-</sup> mice (*P* < 0.01 compared with untreated GPx-1<sup>-/-</sup> controls). This indicates that increasing intracellular thiol pools (principally glutathione) decreases the amount of oxidant stress present with GPx-1<sup>-/-</sup> deficiency and may contribute to the normalization of endothelial function seen after OTC treatment by minimizing oxidative inactivation of NO.

In summary, mice with homozygous deficiency of GPx-1 have impaired endothelium-dependent vascular reactivity in resistance vessels in the presence of increased oxidative and nitrosative stress. Increasing intracellular thiol pools attenuates the increased oxidant stress and reverses the endothelial dysfunction in resistance vessels induced by homozygous deficiency of GPx-1. We conclude that GPx-1 contributes to the maintenance of a normal endothelial function as well as protects against oxidative and nitrosative stress in the blood vessel.

We thank Stephanie Tribuna and Katherine Seropian for assistance in the preparation of this manuscript and Anne Ward Scribner for technical assistance.

This work was supported in part by National Heart, Lung, and Blood Institute (NHLBI) Grants HL-55993, HL-58976, and HL-61795. M. A. Forgione was supported by NHLBI Cardiovascular Training Grant HL-07224-24. N. Weiss was supported by Deutsche Forschungsgemeinschaft Grant WE 1984/2-1.

These results were presented in part at the American Heart Association 72nd Annual Scientific Sessions, November 1999, in Atlanta, GA, and Experimental Biology '99 meeting, April 1999, in Washington, DC.

Present address of N. Weiss: Klinikum der Universität München, Medizinische Poliklinik-Innenstadt, Munich, Germany D-80336.

## REFERENCES

1. **Boesgaard S, Aldershvile J, Poulsen HE, Loft S, Anderson ME, and Meister A.** Nitrate tolerance in vivo is not associated with depletion of arterial or venous thiol levels. *Circ Res* 74: 115–120, 1994.
2. **Bossaller C, Habib GB, Yamamoto H, Williams C, Wells S, and Henry PD.** Impaired muscarinic endothelium-dependent relaxation and cyclic guanosine 5'-monophosphate formation in atherosclerotic human coronary artery and rabbit aorta. *J Clin Invest* 79: 170–174, 1987.
3. **Cheng WH, Ho YS, Valentine BA, Ross DA, Combs GF Jr, and Lei XG.** Cellular glutathione peroxidase is the mediator of body selenium to protect against paraquat lethality in transgenic mice. *J Nutr* 128: 1070–1076, 1998.
4. **Davi G, Alessandrini P, Mezzetti A, Minotti G, Bucciarelli T, Costantini F, Cipollone F, Bon GB, Ciabattini G, and Patrono C.** In vivo formation of 8-epi-prostaglandin F<sub>2</sub> alpha is increased in hypercholesterolemia. *Arterioscler Thromb Vasc Biol* 17: 3230–3235, 1997.
5. **Davi G, Ciabattini G, Consoli A, Mezzetti A, Falco A, Santarone S, Pennese E, Vitacolonna E, Bucciarelli T, Costantini F, Capani F, and Patrono C.** In vivo formation of 8-iso-prostaglandin F<sub>2</sub>alpha and platelet activation in diabetes mellitus: effects of improved metabolic control and vitamin E supplementation. *Circulation* 99: 224–229, 1999.
6. **Dobrina A and Patriarca P.** Neutrophil-endothelial cell interaction. Evidence for and mechanisms of the self-protection of bovine microvascular endothelial cells from hydrogen peroxide-induced oxidative stress. *J Clin Invest* 78: 462–471, 1986.
7. **Eberhardt RT, Forgione MA, Cap A, Leopold JA, Rudd MA, Trolliet M, Heydrick S, Stark R, Klings ES, Moldovan NI, Yaghoubi M, Goldschmidt-Clermont PJ, Farber HW, Cohen R, and Loscalzo J.** Endothelial dysfunction in a murine model of mild hyperhomocyst(e)inemia. *J Clin Invest* 106: 483–491, 2000.
8. **Esposito LA, Kokoszka JE, Waymire KG, Cottrell B, MacGregor GR, and Wallace DC.** Mitochondrial oxidative stress in mice lacking the glutathione peroxidase-1 gene. *Free Radic Biol Med* 28: 754–766, 2000.
9. **Flohé L and Günzler WA.** Assays of glutathione peroxidase. *Methods Enzymol* 105: 114–121, 1984.
10. **Hammerman SI, Klings ES, Hendra KP, Upchurch GR Jr, Rishikof DC, Loscalzo J, and Farber HW.** Endothelial cell

- nitric oxide production in acute chest syndrome. *Am J Physiol Heart Circ Physiol* 277: H1579–H1592, 1999.
11. **Ho YS, Magnenat JL, Bronson RT, Cao J, Gargano M, Sugawara M, and Funk CD.** Mice deficient in cellular glutathione peroxidase develop normally and show no increased sensitivity to hyperoxia. *J Biol Chem* 272: 16644–16651, 1997.
  12. **Jones DP, Eklow L, Thor H, and Orrenius S.** Metabolism of hydrogen peroxide in isolated hepatocytes: relative contributions of catalase and glutathione peroxidase in decomposition of endogenously generated H<sub>2</sub>O<sub>2</sub>. *Arch Biochem Biophys* 210: 505–516, 1981.
  13. **Kurose I, Kubes P, Wolf R, Anderson DC, Paulson J, Miyasaka M, and Granger DN.** Inhibition of nitric oxide production: mechanisms of vascular albumin leakage. *Circ Res* 73: 164–171, 1993.
  14. **Lawson JA, Rokach J, and Fitzgerald GA.** Isoprostanes: formation, analysis and use as indices of lipid peroxidation in vivo. *J Biol Chem* 274: 24441–24444, 1999.
  15. **Levine GN, Keane JF Jr, and Vita JA.** Cholesterol reduction in cardiovascular disease. Clinical benefits and possible mechanisms. *N Engl J Med* 332: 512–521, 1995.
  16. **Marks DS, Vita JA, Folts JD, Keane JF Jr, Welch GN, and Loscalzo J.** Inhibition of neointimal proliferation in rabbits after vascular injury by a single treatment with a protein adduct of nitric oxide. *J Clin Invest* 96: 2630–2638, 1995.
  17. **McAdam BF, Mardini IA, Habib A, Burke A, Lawson JA, Kapoor S, and Fitzgerald GA.** Effect of regulated expression of human cyclooxygenase isoforms on eicosanoid and isoicosanoid production in inflammation. *J Clin Invest* 105: 1473–1482, 2000.
  18. **McLenachan JM, Williams JK, Fish RD, Ganz P, and Selwyn AP.** Loss of flow-mediated endothelium-dependent dilation occurs early in the development of atherosclerosis. *Circulation* 84: 1273–1278, 1991.
  19. **O'Donnell VB and Freeman BA.** Interactions between nitric oxide and lipid oxidation pathways. *Circ Res* 88: 12–21, 2000.
  20. **Palmer RM, Ferrige AG, and Moncada S.** Nitric oxide release accounts for the biological activity of endothelium-derived relaxing factor. *Nature* 327: 524–526, 1987.
  21. **Porta P, Aebi S, Summer K, and Lauterburg BH.** L-2-Oxothiazolidine-4-carboxylic acid, a cysteine prodrug: pharmacokinetics and effects on thiols in plasma and lymphocytes in human. *J Pharmacol Exp Ther* 257: 331–334, 1991.
  22. **Pratico D.** F(2)-isoprostanes: sensitive and specific non-invasive indices of lipid peroxidation in vivo. *Atherosclerosis* 147: 1–10, 1999.
  23. **Quyyumi AA, Dakak N, Anrews NP, Husain S, Arora S, Gilligan DM, Panza JA, and Cannon RO III.** Nitric oxide activity in the human coronary circulation. Impact of risk factors for coronary atherosclerosis. *J Clin Invest* 95: 1747–1755, 1995.
  24. **Raes M, Michiels C, and Remacle J.** Comparative study of the enzymatic defense systems against oxygen-derived free radicals: the key role of glutathione peroxidase. *Free Radic Biol Med* 3: 3–7, 1987.
  25. **Reilly M, Delanty N, Lawson JA, and Fitzgerald GA.** Modulation of oxidant stress in vivo in chronic cigarette smokers. *Circulation* 94: 19–25, 1996.
  26. **Reilly MP, Pratico D, Delanty N, DiMinno G, Tremoli E, Rader D, Kapoor S, Rokach J, Lawson J, and Fitzgerald GA.** Increased formation of distinct F<sub>2</sub> isoprostanes in hypercholesterolemia. *Circulation* 98: 2822–2828, 1998.
  27. **Rosenblat M and Aviram M.** Macrophage glutathione content and glutathione peroxidase activity are inversely related to cell-mediated oxidation of LDL: in vitro and in vivo studies. *Free Radic Biol Med* 24: 305–317, 1998.
  28. **Ross R.** Atherosclerosis—an inflammatory disease. *N Engl J Med* 340: 115–126, 1999.
  29. **Rubbo H and Freeman BA.** Nitric oxide regulation of lipid oxidation reactions: formation and analysis of nitrogen-containing oxidized lipid derivatives. *Methods Enzymol* 269: 385–394, 1996.
  30. **Rubbo H, Radi R, Trujillo M, Telleri R, Kalyanaraman B, Barnes S, Kirk M, and Freeman BA.** Nitric oxide regulation of superoxide and peroxynitrite-dependent lipid peroxidation. Formation of novel nitrogen-containing oxidized lipid derivatives. *J Biol Chem* 269: 26066–26075, 1994.
  31. **Schachinger V, Britten MB, and Zeiher AM.** Prognostic impact of coronary vasodilator dysfunction on adverse long-term outcome of coronary heart disease. *Circulation* 101: 1899–1906, 2000.
  32. **Shwaery GT, Samii JM, Frei B, and Keane JF Jr.** Determination of phospholipid oxidation in cultured cells. *Methods Enzymol* 300: 51–57, 1999.
  33. **Sies H, Sharov VS, Klotz LO, and Briviba K.** Glutathione peroxidase protects against peroxynitrite-mediated oxidations. A new function for selenoproteins as peroxynitrite reductase. *J Biol Chem* 272: 27812–27817, 1997.
  34. **Suwaidi JA, Hamasaki S, Higano ST, Nishimura RA, Holmes DR Jr, and Lerman A.** Long-term follow-up of patients with mild coronary artery disease and endothelial dysfunction. *Circulation* 101: 948–954, 2000.
  35. **Suzuki H, Zweifach BW, and Schmid-Schonbein GW.** Vasodilator response of mesenteric arterioles to histamine in spontaneously hypertensive rats. *Hypertension* 26: 397–400, 1995.
  36. **Upchurch GR Jr, Welch GN, Fabian AJ, Freedman JE, Johnson JL, Keane JF Jr, and Loscalzo J.** Homocyst(e)ine decreases bioavailable nitric oxide by a mechanism involving glutathione peroxidase. *J Biol Chem* 272: 17012–17017, 1997.
  37. **Ursini F, Maiorino M, Brigelius-Flohe R, Aumann KD, Roveri A, Schomburg D, and Flohe L.** Diversity of glutathione peroxidases. *Methods Enzymol* 252: 38–53, 1995.
  38. **Vita JA, Frei B, Holbrook M, Gokce N, Leaf C, and Keane JF Jr.** L-2-Oxothiazolidine-4-carboxylic acid reverses endothelial dysfunction in patients with coronary artery disease. *J Clin Invest* 101: 1408–1414, 1998.
  39. **Weiss N, Zhang Y, and Loscalzo J.** Homocyst(e)ine impairs cellular glutathione peroxidase expression and promotes endothelial dysfunction in an animal model of hyperhomocyst(e)inemia (Abstract). *Circulation* 102: II-238, 2000.
  40. **Williamson JM, Boettcher B, and Meister A.** Intracellular cysteine delivery system that protects against toxicity by promoting glutathione synthesis. *Proc Natl Acad Sci USA* 79: 6246–6249, 1982.
  41. **Williamson JM and Meister A.** Stimulation of hepatic glutathione formation by administration of L-2-oxothiazolidine-4-carboxylate, a 5-oxo-L-proline substrate. *Proc Natl Acad Sci USA* 78: 936–939, 1981.